Supplementary Material (ESI) for Chemical Communications

Supporting Information

The Bis(Hydrogenheptaphosphide)iron(II) dianion: a Zintl ion analogue of ferrocene.

Caroline Knapp, Joseph S. Large, Nicholas H. Rees and Jose M. Goicoechea*

Department of Chemistry, Chemistry Research Laboratory, University of Oxford, Mansfield Road, Oxford, OX1 3TA, U.K.

1. Experimental Section

General synthetic methods. All reactions and product manipulations were carried out under an inert atmosphere using standard Schlenk-line or glovebox techniques (MBraun UNIlab glovebox maintained at < 0.1 ppm H_2O and < 0.1 ppm O_2). The Zintl phase precursor K_3P_7 was synthesised according to a previously reported synthetic procedure from a mixture of the elements (K: 99.95%, Aldrich; P: 99.99%, Aldrich).[1] Anhydrous $FeCl_2$ (98%, Strem) was used as received. 2,2,2-crypt (4,7,13,16,21,24-hexaoxa-1,10-diazabicyclo[8.8.8]hexacosane; 99+%, Merck) was also used as received after careful drying under vacuum. Toluene (tol; 99.9%, Rathburn), tetrahydrofuran (THF; 99.9%, Rathburn) and dimethylformamide (DMF; 99.9%, Rathburn) were purified using an MBraun SPS-800 solvent system. Ethylenediamine (en; 99%, Aldrich) and pyridine (py; 99.9%, Rathburn) were distilled over sodium metal and CaH_2, respectively. d_5-Pyridine (99.5%, Cambridge Isotope Laboratories, Inc.) was dried over CaH_2 and vacuum distilled. All solvents were stored under argon in gas-tight ampoules. In addition toluene was stored over activated 3 Å molecular sieves (Acros).

$[K(2,2,2\text{-crypt})]_2[Fe(HP_7)_2]$ (**1**): K_3P_7 (123 mg, 0.37 mmol), $FeCl_2$ (30 mg, 0.24 mmol), $[NH_4][B(C_6H_5)_4]$ (95 mg, 0.28 mmol) and 2,2,2-crypt (228 mg, 0.61 mmol) were dissolved in approximately 3 mL of ethylenediamine and left to stir under argon for 3 hours. The resulting reddish-black solution was reduced to dryness under a dynamic vacuum yielding a dark brown residue. This solid was washed twice with approximately 10 mL of THF and sonicated in an effort to dissolve the chloride and tetraphenylborate salt by-products. The THF fractions were filtered off and disposed off and the remaining solid residue dried under vacuum

yielding 184 mg (76% yield) of a dark brown solid. X-ray quality crystals of **1** were grown from a pyridine/toluene solvent mixture. Anal. Calcd for $C_{36}H_{74}FeK_2N_4O_{12}P_{14}$: C, 32.69; H, 5.64; N, 4.24. Found: C, 32.39; H, 5.47; N, 4.18. ^{1}H NMR (500 MHz, d_5-pyridine): δ(ppm) 6.54 (d, $^1J(H,P)$=169 Hz, 1H: H1,1A), 3.47 (br s, 12H: 2,2,2-crypt), 3.42 (br s, 12H: 2,2,2-crypt), 2.41 (br s, 12H: 2,2,2-crypt); ^{31}P NMR (202.4 MHz, d_5-pyridine): δ(ppm) 151.1 ppm (dt, $^1J(P,P)$=267 Hz, $^1J(H,P)$=169 Hz, 1P: P1,1A), –0.7 (m, 2P; P2,3,2A,3A), –80.6 (m, 2P: P4,5,4A,5A/P6,7,6A,7A), –121.5 (m, 2P; P6,7,6A,7A/P4,5,4A,5A). ESI– MS (DMF): *m/z* 491.6 $[Fe(HP_7)_2]^-$, 907.0 $\{[K(2,2,2\text{-crypt})][Fe(HP_7)_2]\}^-$. ESI+ MS (DMF): *m/z* 1737.0 $\{[K(2,2,2\text{-crypt})]_3[Fe(HP_7)_2]\}^+$, 2151.2 $\{[K(2,2,2\text{-crypt})]_4[Fe(HP_7)_2]\}^+$.

Single crystal X-ray structure determination: Single-crystal X-ray diffraction data were collected using an Enraf-Nonius Kappa-CCD diffractometer and a 95 mm CCD area detector with a graphite-monochromated molybdenum K_α source (λ = 0.71073 Å). Crystals were selected under Paratone-N oil before being mounted on fibres and positioned under a nitrogen stream. Nitrogen flow temperatures were controlled by an Oxford Cryosystems cryostat. Equivalent reflections were merged and diffraction patterns processed with the DENZO and SCALEPACK programs.[2] The structure was subsequently solved using direct methods, and refined on F^2 using the SHELXL 97-2 package.[3] CCDC-794183 contains the supplementary crystallographic data for **1**.

1: Formula: $C_{36}H_{74}FeK_2N_4O_{12}P_{14}$; M_r = 1322.62; crystal colour and morphology: small orange plates; crystal size: 0.14 × 0.10 × 0.05 mm; triclinic; space group: *P-1*; a = 10.9876(3) Å; b = 12.1241(4) Å; c = 12.7331(6) Å; α = 66.710(1)°; β = 84.955(1)°; γ = 73.754(2)°; V = 1495.31(10) Å^3; Z = 1; ρ_{calcd} = 1.469 g cm^{-3}; μ = 0.820 mm^{-1}; T = 150(2) K; 8683 reflections collected; 5154 independent reflections; R_{int} = 0.0427; R_1 = 4.27 and R_2 = 8.63 for $I \geq 2\sigma(I)$; R_1 = 7.57 and R_2 = 10.00 for all data.

Other characterization techniques: Positive and negative ion mode electrospray mass spectra were recorded on DMF solutions (10–20 mm) on a Masslynx LCT Time of Flight mass spectrometer with a Z-spray source (150°C source temperature, 200°C desolvation temperature, 2.4 kV capillary voltage and 25 V cone voltage). The samples were made up inside a glovebox under an inert atmosphere and rapidly transferred to the spectrometer in an air-tight syringe. Samples were introduced directly with a 1 mL SGE syringe and a syringe pump at 0.6 mL h^{-1}.

^{1}H and ^{31}P NMR spectra were acquired at 500.0 and 202.4 MHz, respectively, on a Varian Unity-plus 500 NMR spectrometer. ^{1}H spectra were referenced to the most upfield residual protic solvent resonance (pyridine δ 7.22 ppm). ^{31}P spectra were externally referenced to H_3PO_4 (δ 0 ppm). Spectral simulations were carried out using the program gNMR.[4]

Elemental analyses were carried out by Stephen Boyer of the London Metropolitan University Samples (approx. 5 mg) were submitted in sealed Pyrex ampoules.

[1] (a) Corbett, J. D.; Adolphson, D. G.; Merryman, D. J.; Edwards, P. A.; Armatis, F. J. *J. Am. Chem. Soc.* **1975**, *97*, 6267. (b) Emmerling, F.; Röhr, C. *Z. Naturforsch.* **2002**, *57b*, 963. (c) Santandrea, R. P.; Mensing, C.; von Schnering, H. G. *Thermochim. Acta* **1986**, *98*, 301.

[2] Otwinowski, Z.; Minor, W. *Processing of X-ray Diffraction Data Collected in Oscillation Mode*, Academic Press: New York, 1997.

[3] (a) Sheldrick, G. M. *Acta Crystallogr. Sect. A* **1990**, *46*, 467. (b) SHELX97, *Programs for Crystal Structure Analysis (Release 97–2)*, Sheldrick, G. M. University of Göttingen (Germany), 1998.

[4] NMR spectra simulated using: gNMR v5.0, Budzelaar, P. H. M., 1995-2006, IvorySoft.

2. Computed structures and analysis of electronic structure

2.1 Computational details

All calculations described in this paper were performed using the Amsterdam Density Functional package (ADF2007.01).[5] A triple-ζ Slater-type basis set, extended with a single polarization function, was used to describe all atoms. The local density approximation was employed for the optimizations,[6] along with the local exchange-correlation potential of Vosko, Wilk and Nusair[7] and the gradient corrections to exchange and correlation proposed by Becke and Perdew (BP86).[8] Relativistic effects were incorporated using the Zeroth Order Relativistic Approximation (ZORA).[9] The presence of cations in the crystal lattice of **1** was modelled by surrounding the anion with a continuum dielectric using COSMO.[10] The chosen dielectric constant $\varepsilon = 16.9$ corresponds to that of ammonia, although structural parameters are not strongly dependent on this choice. All structures were optimized using the gradient algorithm of Versluis and Ziegler.[11]

[5] (a) te Velde, G.; Bickelhaupt, F. M.; Baerends, E. J.; Fonseca Guerra, C.; van Gisbergen, S. J. A.; Snijders, J. G.; Ziegler, T. *J. Comput. Chem*. **2001**, *22*, 931. (b) Fonseca Guerra, C.; Snijders, J. G.; te Velde G.; Baerends, E. J. *Theor. Chem. Acc*. **1998**, *99*, 391. (c) ADF 2008.01, SCM, Theoretical Chemistry, Vrije Universiteit, Amsterdam, The Netherlands, http://www.scm.com.

[6] Parr R. G.; Yang, W. *Density Functional Theory of Atoms and Molecules*, Oxford University Press: Oxford, 1989.

[7] Vosko, S. H.; Wilk, L.; Nusair, M. *Can. J. Phys*. **1980**, *58*, 1200.

[8] (a) Becke, A. D. *Phys. Rev. A* **1988**, *38*, 3098. (b) Perdew, J. P. *Phys. Rev. B* **1986**, *33*, 8822.

[9] (a) van Lenthe, E.; Baerends, E. J.; Snijders, J. G. *J. Chem. Phys*. **1993**, *99*, 4597. (b) van Lenthe, E.; Baerends E. J.; Snijders, J. G. *J. Chem. Phys*. **1994**, *101*, 9783. (c) van Lenthe, E.; Ehlers, A.; Baerends, E. J. *J. Chem. Phys*. **1999**, *110*, 8943.

[10] Klamt, A. *J. Phys. Chem.* **1995**, 2224.

[11] Versluis L.; Ziegler, T. *J. Chem. Phys*. **1988**, *88*, 322.

Cartesian coordinates [Å] for the optimized structure of the norbornadiene-like isomer of $[HP_7]^{2-}$

Atom	x	y	z
P1	–0.612522	2.004977	0.000000
P2	–0.240560	0.574797	–1.677158
P3	–0.240560	0.574797	1.677158
P4	1.746484	–0.141037	–1.084488
P5	1.746484	–0.141037	1.084488
P6	–1.126080	–1.348493	–1.075277
P7	–1.126080	–1.348493	1.075277
H1	–2.042863	1.892607	0.000000

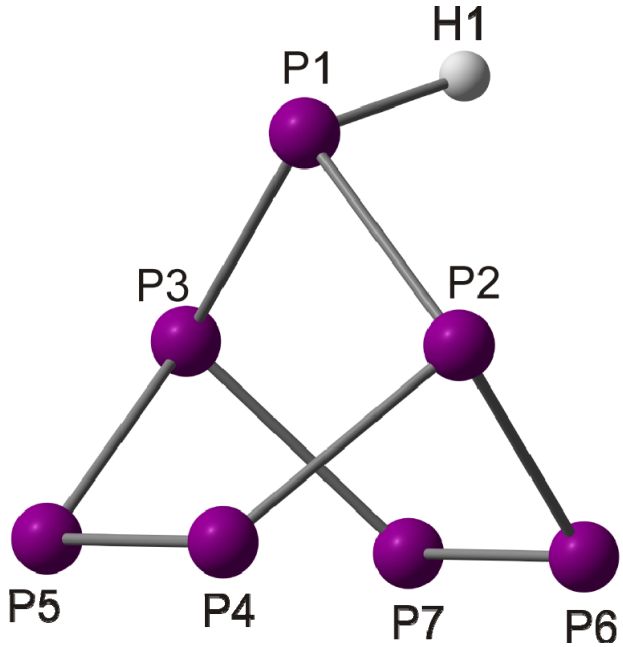

Figure S1. Optimized geometry of the norbornadiene-like isomer of the $[HP_7]^{2-}$ cluster anion from DFT calculations.

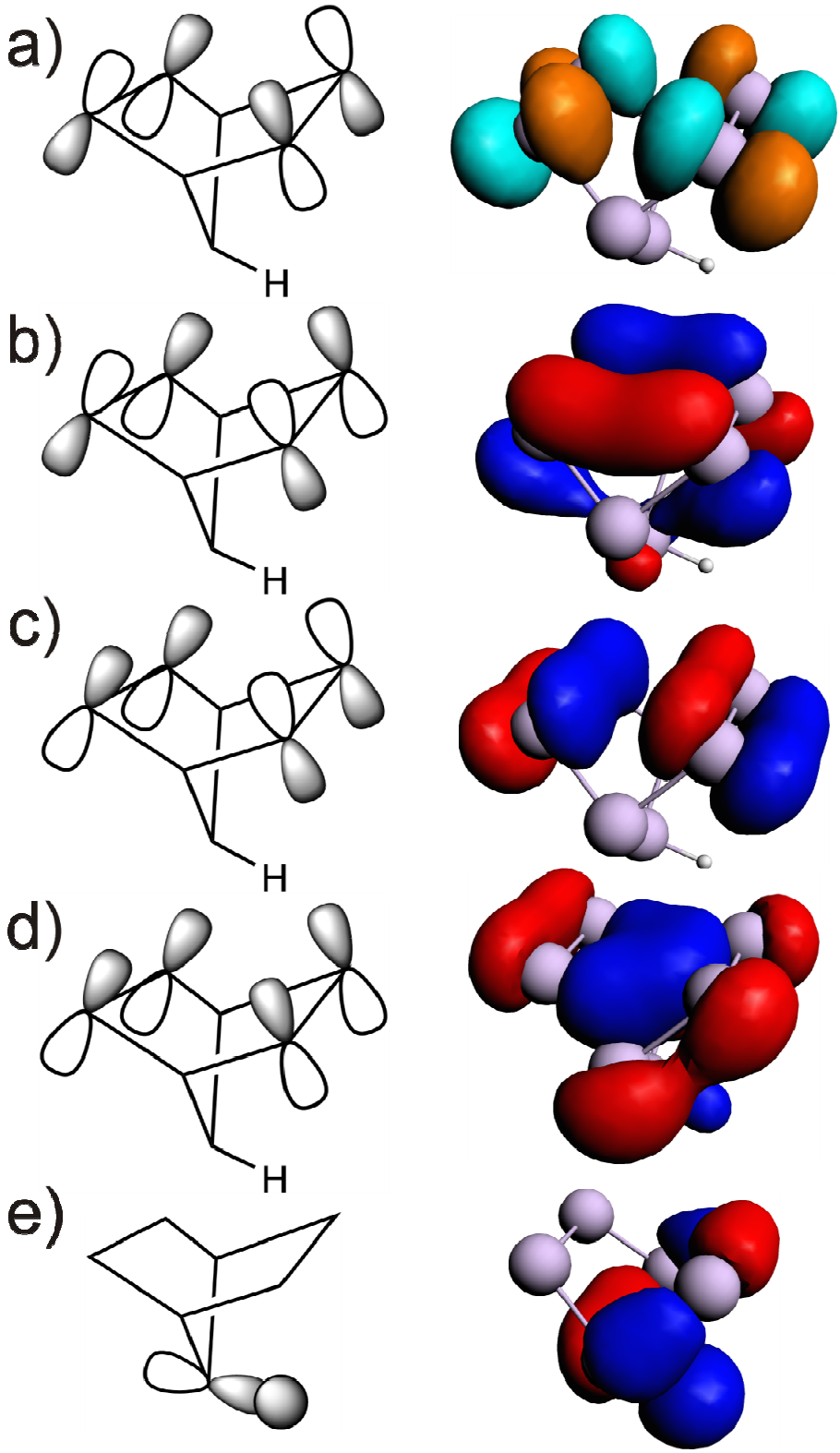

Figure S2. Selected frontier orbitals for the optimized structure of the $[HP_7]^{2-}$ anion. a) LUMO b) HOMO, c) HOMO – 1, d) HOMO – 9, e) HOMO – 11.

Cartesian coordinates [Å] for the optimized structure of *staggered* $[Fe(HP_7)_2]^{2-}$

Atom	x	y	z
Fe1	0.000000	0.000000	0.000000
P1	0.037816	0.371658	4.423898
P2	–1.678297	0.059825	3.065422
P3	1.724140	0.026016	3.040191
P4	–1.089812	1.523059	1.452430
P5	1.101632	1.517585	1.484160
P6	–1.068879	–1.478804	1.550033
P7	1.096611	–1.488778	1.485973
H1	0.017708	–0.905890	5.083853
P1A	0.261063	0.261733	–4.420870
P2A	1.278335	–1.139015	–3.050936
P3A	–1.225067	1.161861	–3.064470
P4A	–0.225192	–1.826987	–1.532797
P5A	–1.811586	–0.354790	–1.492939
P6A	1.839142	0.349065	–1.448929
P7A	0.234367	1.842377	–1.501259
H1A	–0.581997	–0.677482	–5.113691

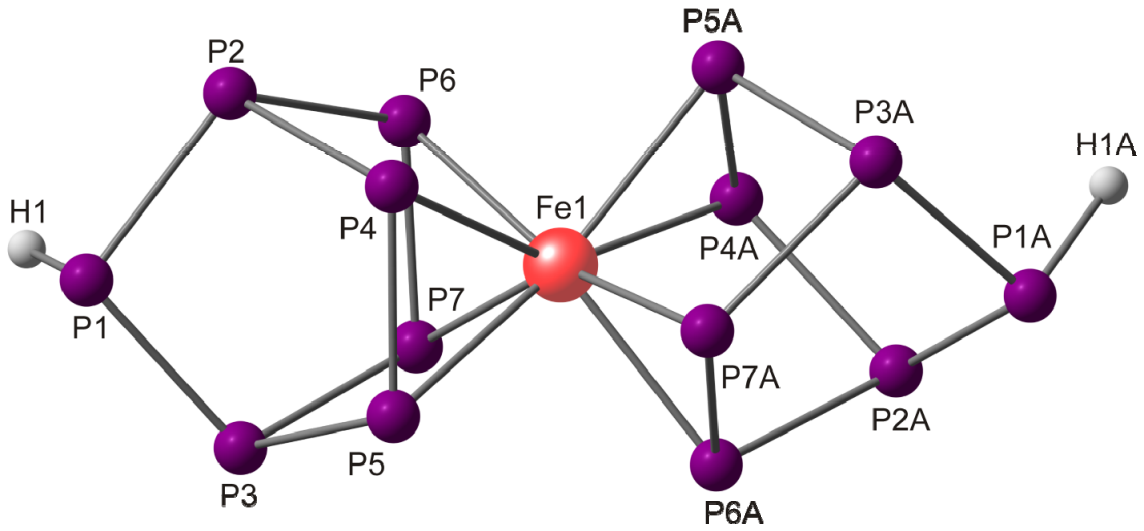

Figure S3. Optimized geometry of the staggered isomer of the $[Fe(HP_7)_2]^{2-}$ cluster anion from DFT calculations.

Cartesian coordinates [Å] for the optimized structure of *eclipsed* $[Fe(HP_7)_2]^{2-}$

Atom	x	y	z
Fe	0.000000	0.000000	0.000000
P1	0.158366	–0.191586	–4.508978
P2	–1.592919	0.161187	–3.213461
P3	1.811160	0.006541	–3.065380
P4	–1.113011	–1.365328	–1.631619
P5	1.062500	–1.483228	–1.558274
P6	–0.973849	1.551236	–1.552367
P7	1.179231	1.478562	–1.484512
H1A	0.241936	1.104376	–5.126068
P1A	–0.158366	0.191586	4.508978
P2A	1.592919	–0.161187	3.213461
P3A	–1.811160	–0.006541	3.065380
P4A	1.113011	1.365328	1.631619
P5A	–1.062500	1.483228	1.558274
P6A	0.973849	–1.551236	1.552367
P7A	–1.179231	–1.478562	1.484512
H1A	–0.241936	–1.104376	5.126068

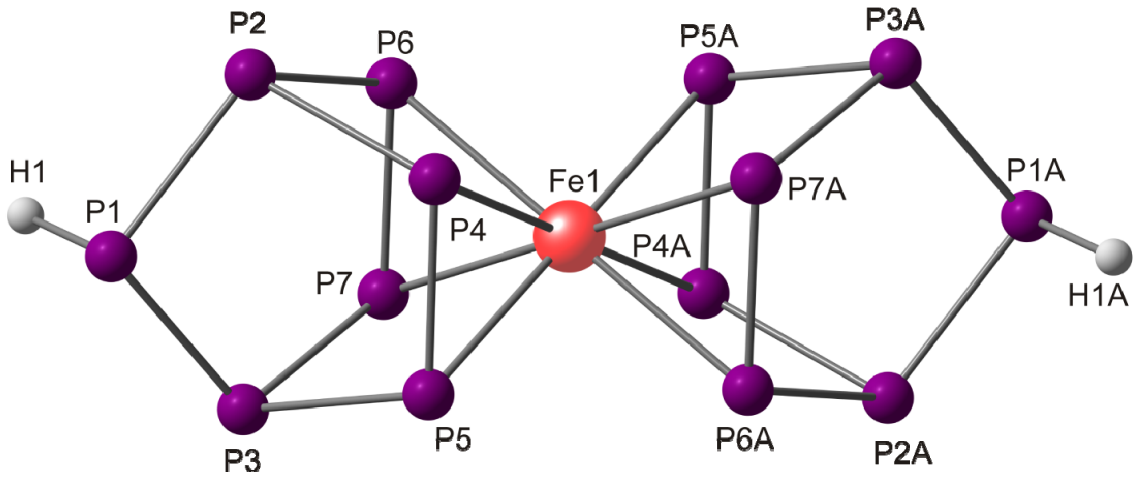

Figure S4. Optimized geometry of the eclipsed isomer of the $[Fe(HP_7)_2]^{2-}$ cluster anion from DFT calculations.

Table S1. Interatomic distances [Å] for the $[Fe(HP_7)_2]^{2-}$ cluster anion crystallographically characterized in **1** and for the optimized computed structures.

bond	**1**	***staggered* isomer**	***eclipsed* isomer**
Fe1-P4	2.370 (2)	2.367	2.401
Fe1-P5	2.412(2)	2.388	2.399
Fe1-P6	2.464(2)	2.395	2.401
Fe1-P7	2.486(2)	2.374	2.404
P1-P2	2.051(7)	2.208	2.207
P1-P3	2.208(6)	2.204	2.203
P2-P4	2.215(2)	2.257	2.251
P2-P6	2.206(3)	2.245	2.253
P3-P5	2.206(3)	2.244	2.248
P3-P7	2.218(3)	2.261	2.251
P4-P5	2.135(2)	2.193	2.180
P6-P7	2.149(3)	2.164	2.155
P4-P6	3.001(3)	3.001	2.921
P5-P7	3.023(3)	3.002	2.965
P1-H1	1.20(2)	1.440	1.438
Fe1-P4A	2.378(2)	2.394	2.401
Fe1-P5A	2.268(2)	2.372	2.399
Fe1-P6A	2.338(2)	2.370	2.401
Fe1-P7A	2.272(2)	2.392	2.404
P1A-P2A	2.177(8)	2.211	2.207
P1A -P3A	2.222(8)	2.209	2.203
P2A-P4A	2.197(3)	2.244	2.250
P2A-P6A	2.222(3)	2.256	2.253
P3A-P5A	2.206(3)	2.259	2.248
P3A-P7A	2.201(3)	2.244	2.251
P4A-P5A	2.132(3)	2.166	2.180
P6A-P7A	2.153(3)	2.192	2.155
P4A-P6A	3.002(3)	3.004	2.921
P5A-P7A	2.985(3)	3.006	2.965
P1A-H1A	1.07(7)	1.438	1.438

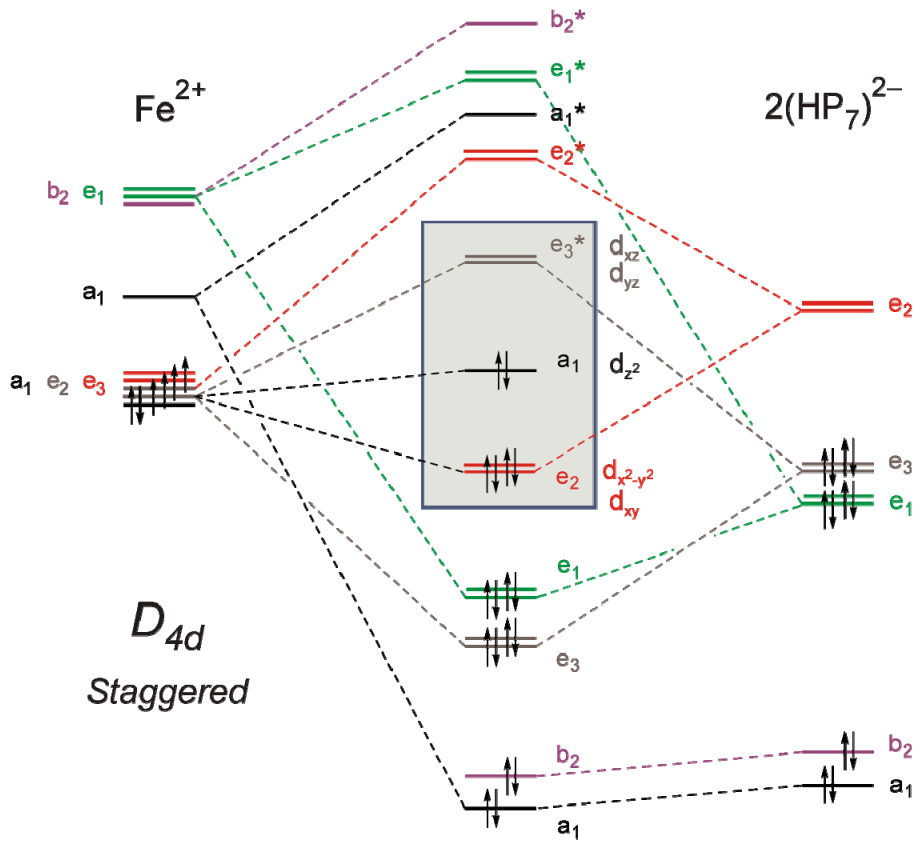

Figure S5. Qualitative molecular orbital diagram for the *staggered*-isomer of $[Fe(HP_7)_2]^{2-}$. An idealized D_{4d} geometry has been assumed to highlight symmetry allowed interactions between metal based orbitals and the symmetry adapted linear combinations (SALC) of the π-manifold frontier orbitals of two $[HP_7]^{2-}$ cages.

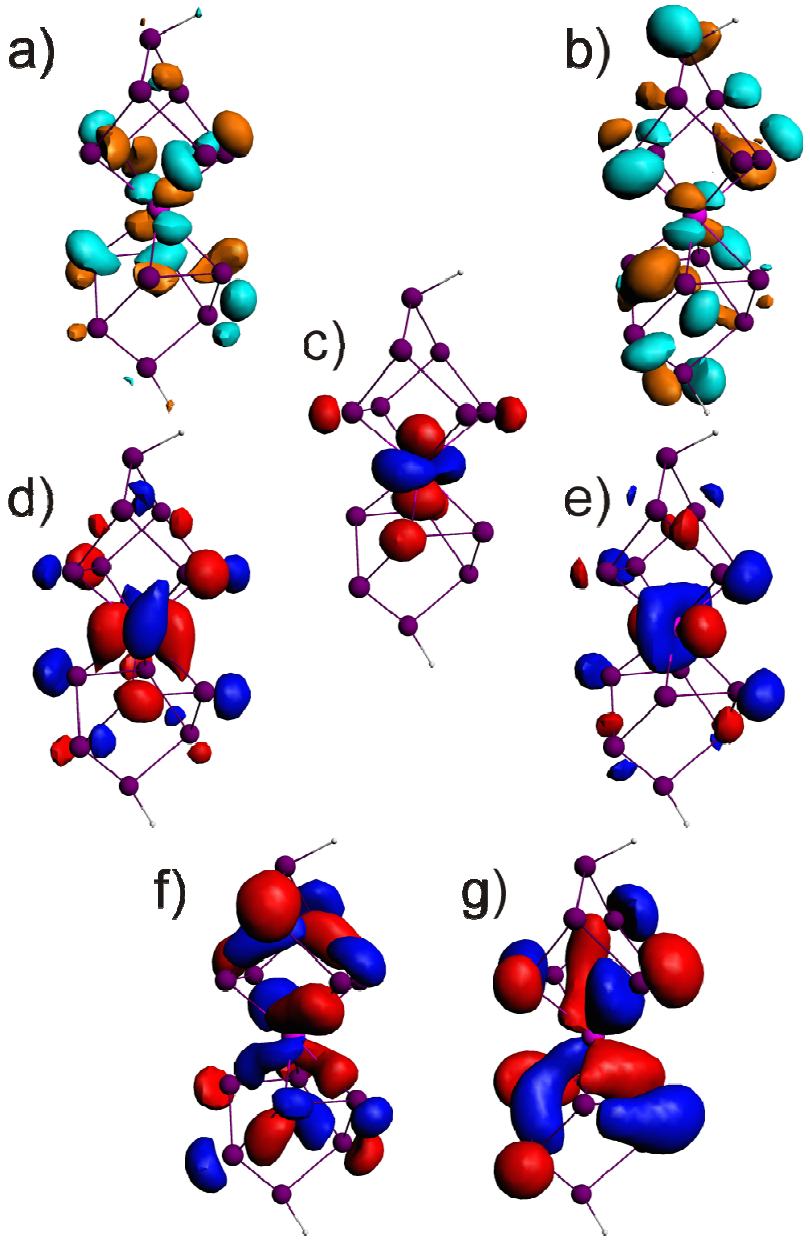

Figure S6. Selected frontier molecular orbitals for the computed optimized geometry of the *staggered*-isomer of $[Fe(HP_7)_2]^{2-}$. a) LUMO; b) LUMO+1; c) HOMO; d) HOMO–1; e) HOMO–2; f) HOMO–4; g) HOMO–11.

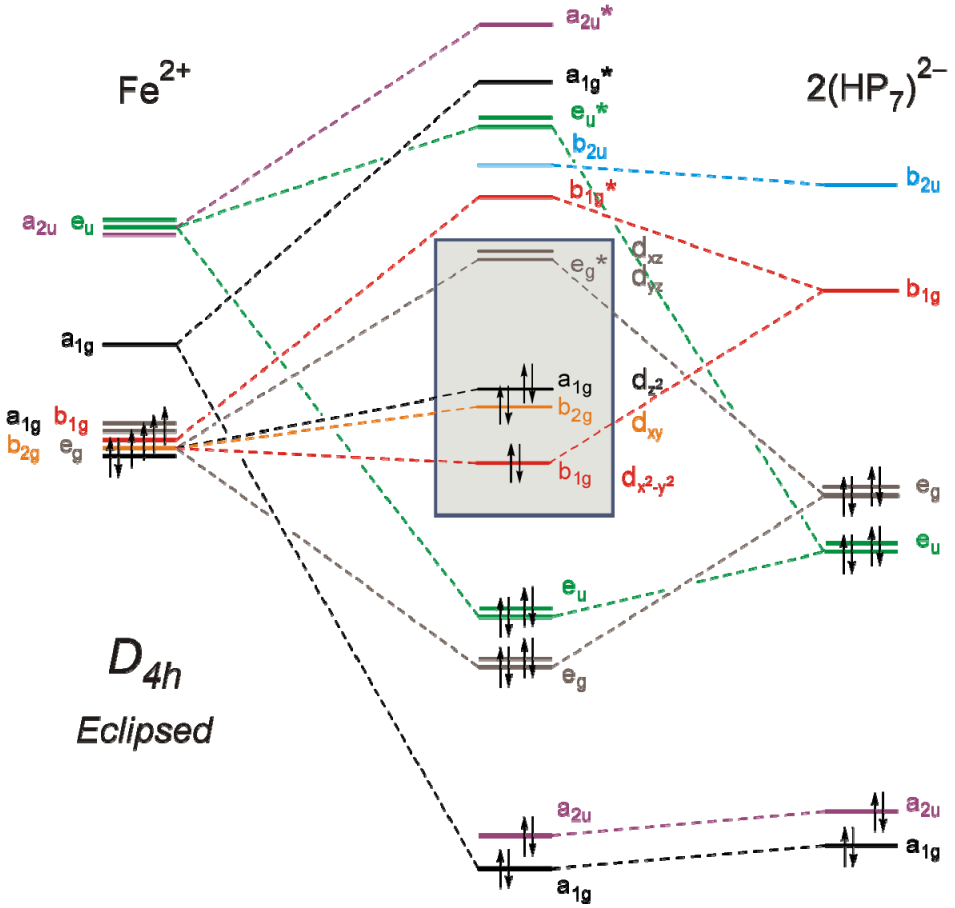

Figure S7. Qualitative molecular orbital diagram for the *eclipsed*-isomer of $[Fe(HP_7)_2]^{2-}$. An idealized D_{4h} geometry has been assumed to highlight symmetry allowed interactions between metal based orbitals and the symmetry adapted linear combinations (SALC) of the π-manifold frontier orbitals of two $[HP_7]^{2-}$ cages.

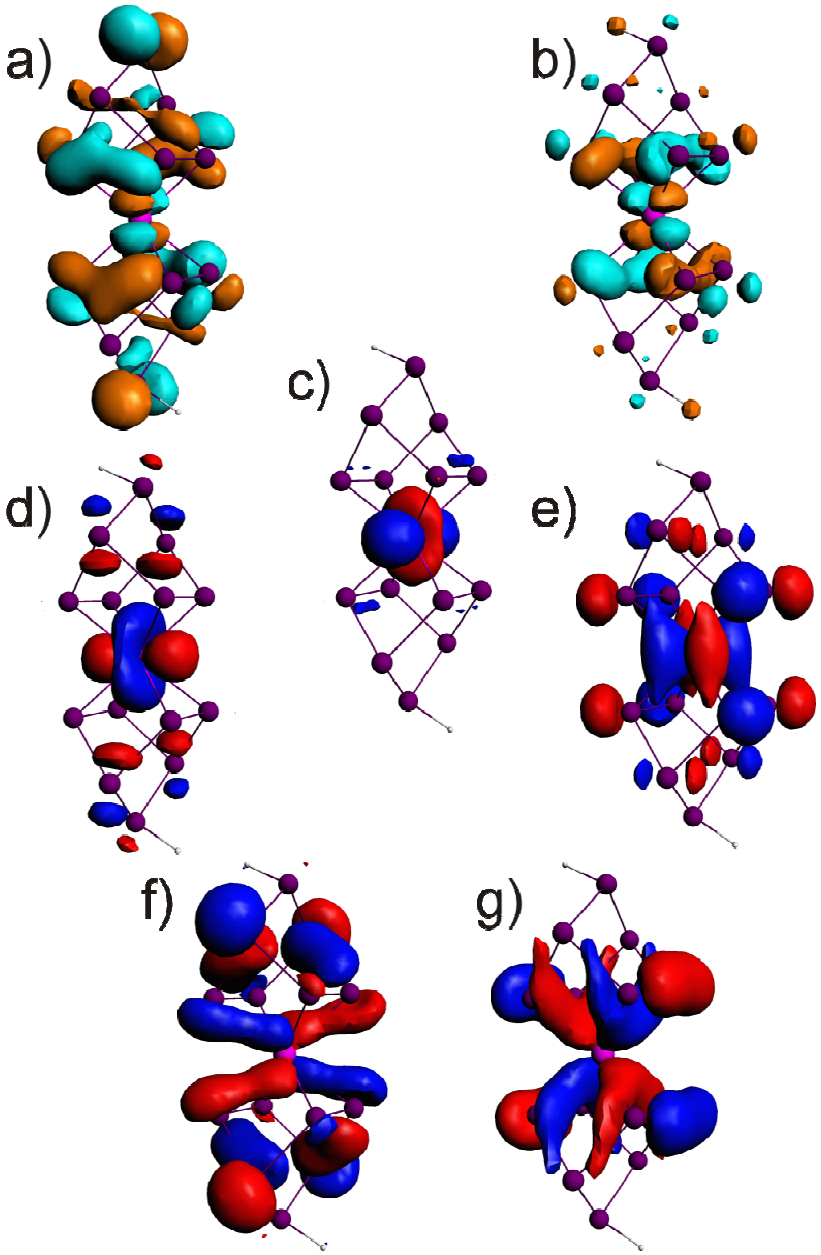

Figure S8. Selected frontier molecular orbitals for the computed optimized geometry of the *eclipsed*-isomer of $[Fe(HP_7)_2]^{2-}$. a) LUMO; b) LUMO+1; c) HOMO; d) HOMO–1; e) HOMO–2; f) HOMO–4; g) HOMO–9.

3. NMR spectra

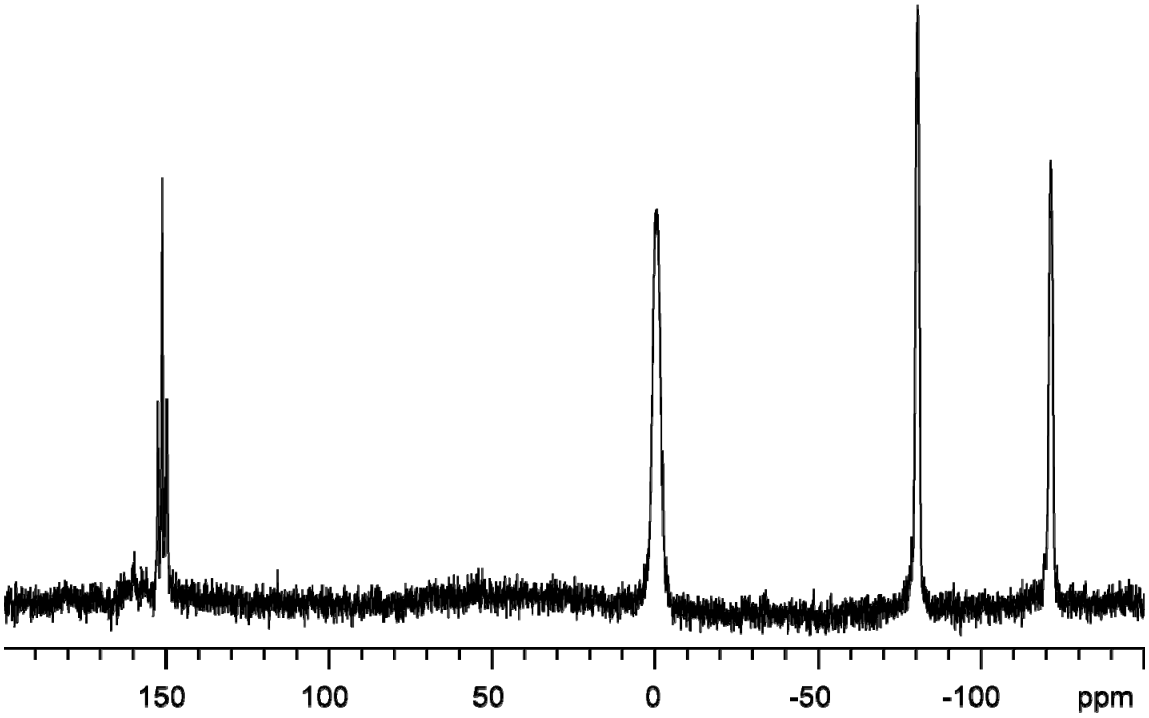

Figure S8. Room temperature $^{31}P\{^{1}H\}$ NMR spectrum of a d_5-pyridine solution of **1**.

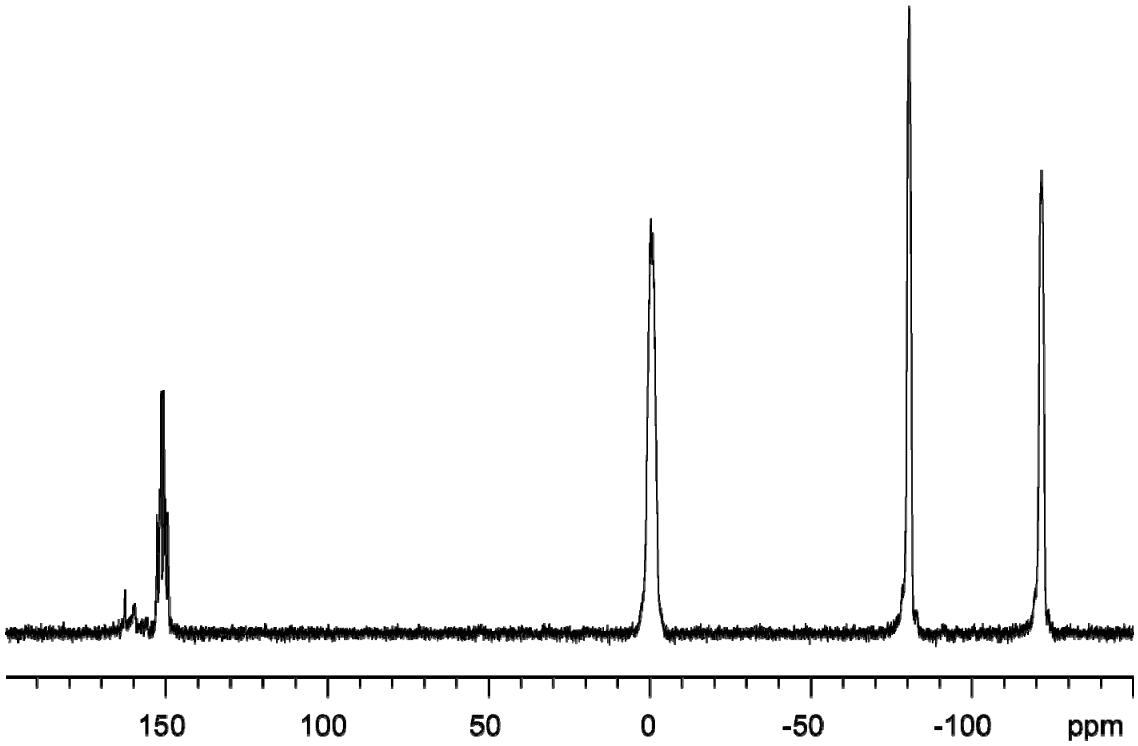

Figure S9. Room temperature ^{31}P NMR spectrum of a d_5-pyridine solution of **1**.

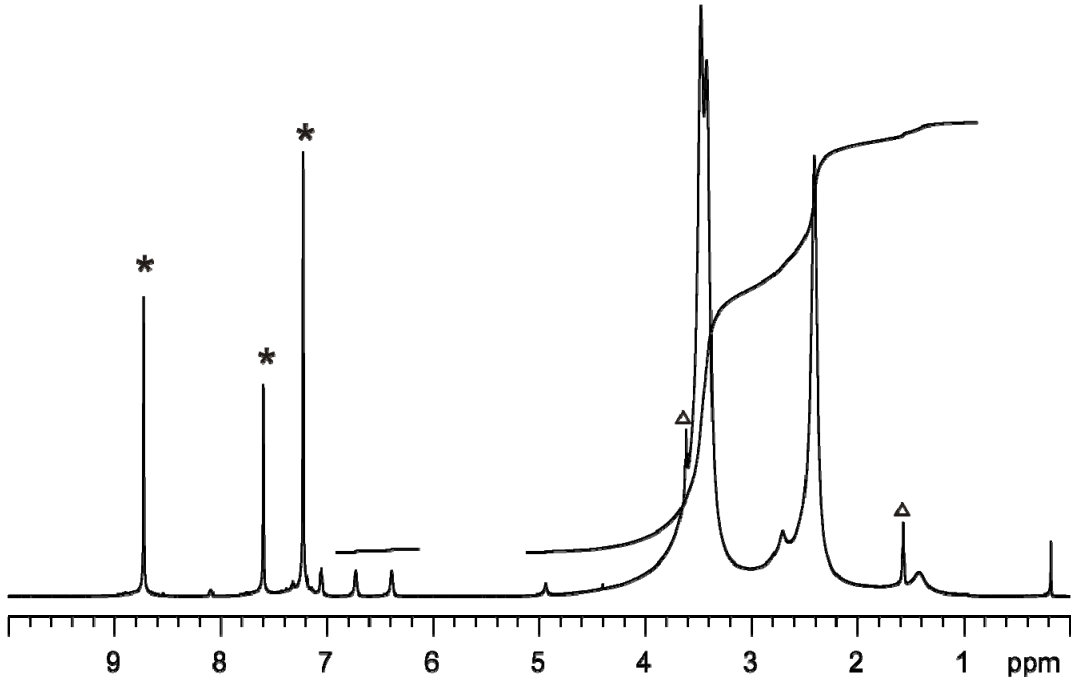

Figure S10. Room temperature ^{1}H NMR spectrum of a d_5-pyridine solution of **1**. Resonances highlighted with an asterisk correspond to protic pyridine whereas those highlighted with a triangle arise from trace amounts of THF.

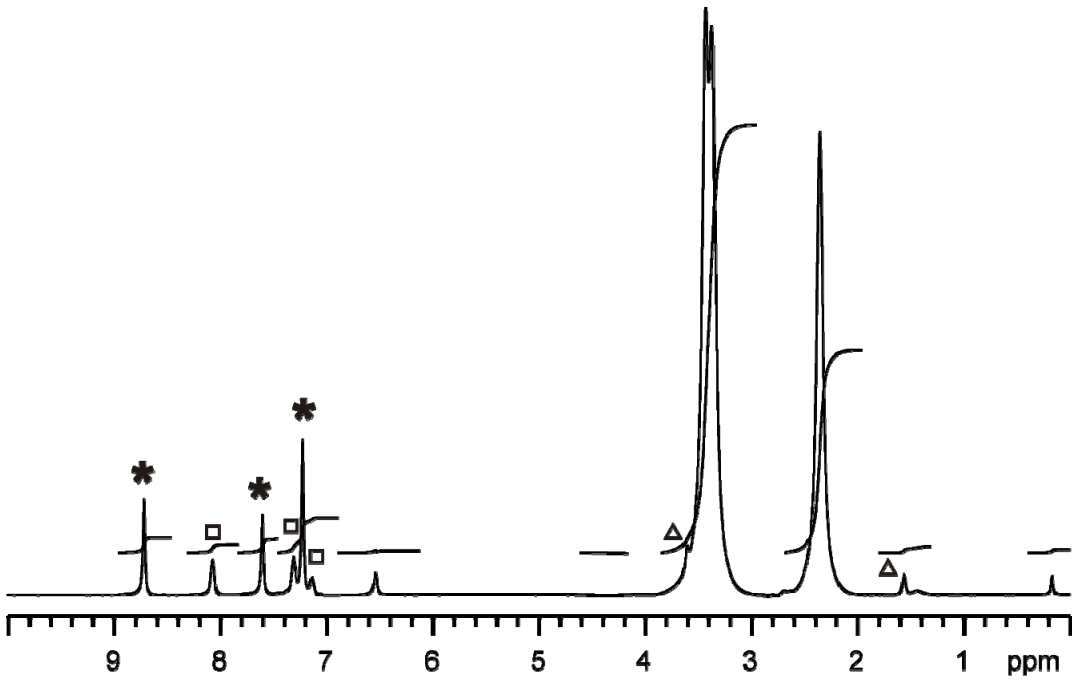

Figure S11. Room temperature $^{1}H\{^{31}P\}$ NMR spectrum of a d_5-pyridine solution of **1**. Resonances highlighted with an asterisk correspond to protic pyridine. Resonances identified with a triangle arise from trace amounts of THF, whereas those with a square correspond to $[B(C_6H_5)_4]^-$.

4. ES-MS spectra

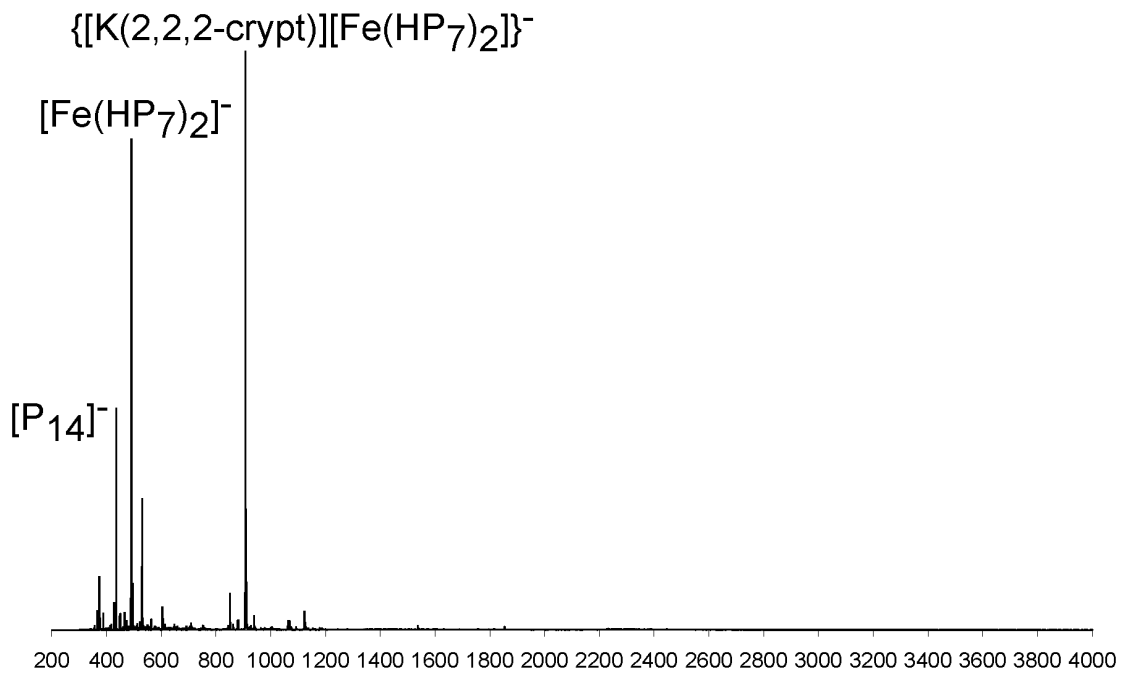

Figure S12. Negative ion mode electrospray mass-spectrum of a DMF solution of **1**.

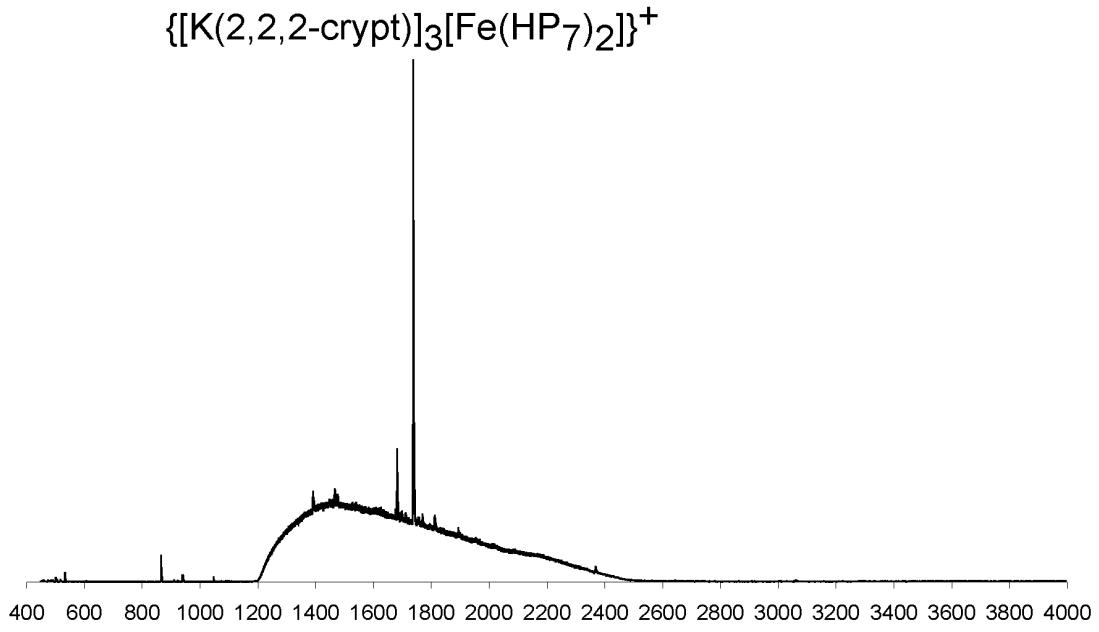

Figure S13. Positive ion mode electrospray mass-spectrum of a DMF solution of **1**.